Least-effort trajectories lead to emergent crowd behaviors

Stephen J. Guy, Sean Curtis, Ming C. Lin, and Dinesh Manocha

Phys. Rev. E **85**, 016110 — Published 17 January 2012

DOI: 10.1103/PhysRevE.85.016110

Least-Effort Trajectories Lead to Emergent Crowd Behaviors

Stephen J. Guy,* Sean Curtis, Ming C. Lin, and Dinesh Manocha
Department of Computer Science, University of North Carolina at Chapel Hill, NC, 27599

Pedestrian crowds have often been modeled as many-particle systems, usually using computer models known as multi-agent simulations. The key challenge in modeling crowds is to develop rules that guide how the particles or agents interact with each other in a way that faithfully reproduces paths and behaviors commonly seen in real human crowds. Here we propose a simple and intuitive formulation of these rules based on biomechanical measurements and the Principle of Least Effort. We present a constrained optimization method to compute collision-free paths of minimum caloric energy for each agent, from which collective crowd behaviors can be reproduced. We show that our method reproduces common crowd phenomena, such as arching and self-organization into lanes. We also validate the flow rates and paths produced by our method and compare them to those of real-world crowd trajectories.

I. INTRODUCTION

Heterogenous crowds consist of people with differing goals and behaviors, but often display interesting and predictable characteristics. Individuals within these crowds, must navigate to their goals despite potentially congested environments and the conflicting paths of others in the crowd. A key observation in understanding how individual trajectories are formulated arises from the well-known Principle of Least Effort, a broad theory which suggests that people naturally choose the path of least effort in order to reach their goals [1]. This principle has been applied to successfully explain human locomotion patterns [2] and predict the velocity range at which individuals generally travel [3, 4]. While much is known about movement and speeds for humans walking in an isolated setting, modeling accurate motions and trajectories for crowds from individual human motion is not well understood [5].

Many researchers, including Hoogendoorn and Bovy [6], have shown that crowd motion can be modeled as independent agents that try to optimize some utility function. In this paper, we show how to extend the classic Principle of Least Effort to model the motion of humans in a crowd using an optimization based framework which captures collective crowd behaviors. We present a novel model based on this principle, which minimizes the total biomechanical effort of each individual moving within a crowd. We combine this model with biomechanical measurements to produce highly efficient computer simulations that compare well with empirical data on human trajectories. Moreover, we show that this model can accurately reproduce many emergent crowd behaviors and numerically predict crowd flows in different settings.

Several models have been proposed to simulate human motion in a crowd. While some methods try to model the macroscopic or overall motion of the crowd [7, 8], our goal is to accurately compute trajectories of individual pedestrians. Therefore we propose a microscopic, or agent-based, model of human motion which specifically tries to model the position and velocity of each individual over time. Previously proposed models of this type include many-particle force-based models [9, 10] and their important extensions [11, 12], methods based on simple rules [13], flow-field based methods [14], and Cellular Automata models [15, 16]. Methods have also been proposed which fit models to recorded data [17] or extended existing models to capture newly recognized phenomena [18]. An overview of this general area of the physics of complex systems and transport can be found in Schadschneider et al. [19]. Recently, researchers have proposed geometric optimization based, multi-agent simulation methods where agents attempt to directly compute collision free velocities in a predictive manner, based on anticipated motion [20], data collected on humans [21], and cognitive theories of perception [22]. Our model likewise uses an optimization framework, which in contrast, is based on biomechanical principles of individual motion.

In this article, we show that our biomechanically based model of pedestrian dynamics model can meaningfully predict the trajectories of humans in crowds and thereby generate natural crowd behaviors. Specifically, we show that individuals in a crowd minimizing their expected caloric expenditure results in a number of common crowd behaviors and phenomena. We denote these behaviors as "emergent behaviors", because they are an indirect result of individuals minimizing the expected energy of their paths. We also show that our model's predictions match the paths and flow rates of real humans. While previous methods have demonstrated some of these aspects, our proposed method can demonstrate all of these aspects and is based on a simple interpretation of human biomechanics.

A key issue in the design of an optimization-based approach is determining the correct metric to optimize. Previous approaches have suggested minimizing the total distance traveled (such as by using differential geometry [24], planning on geodesics[16], or using flow-based techniques [8]). However, path length minimization is not a complete metric as its value is independent of an agent's speed. Additionally, it fails to model important

* sjguy@cs.unc.edu

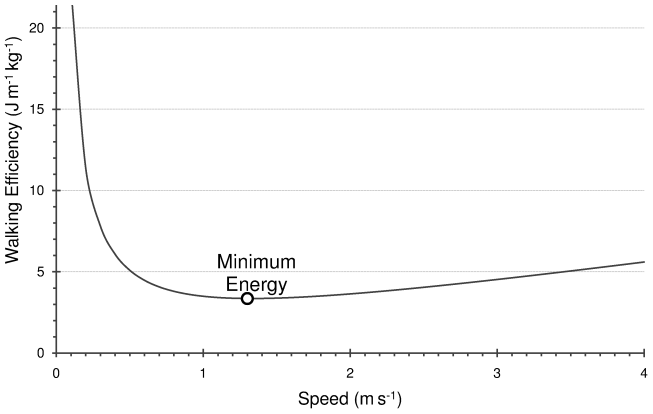

FIG. 1: Graph of the empirical relationship between velocity and caloric efficiency for adult males [4] (Eq. 1). The minimum energy corresponds to the velocity 1.3 m/s, the average walking velocity for adult males. [23]

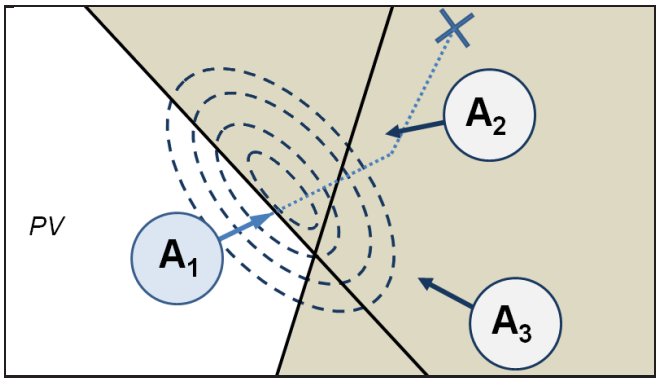

FIG. 2: (Color online) Computation Overview. The current agent, A_1, has a goal marked X, but needs to avoid two approaching agents, A_2 and A_3, each with some velocity (arrows). Each neighbor creates a restriction on the velocity the current agent can take (boundary line and shaded regions show forbidden endpoints of the velocity vector of A_1), leaving the set of collision-free permissible velocities (PV). Each velocity results in some expected energy to reach the goal (dashed ellipses mark the iso-contours of this function). The computed new velocity (light arrow) is the one which leads to the collision-free path to the goal (dotted line) using the least expected energy. This model is used to compute a new velocity for each agent at each simulation time-step.

real-world phenomena such as why humans tend to avoid congestion. In contrast, biomechanics research suggests a natural metric of calories expended over a path.

When walking in an unconstrained environment, people are known to move at velocities that minimize their caloric expenditure per unit distance [3, 4]. However, when in crowd-like settings, other people create constraints on the possible motion an individual can take. We posit that it is this interaction between different individuals, each of whom is independently minimizing his or her expected effort, that gives rise to the emergent behaviors and motion patterns exhibited by crowds. Such behaviors can be numerically approximated by performing a constrained minimization over all the paths each individual can take, as described below. Our model is to compute all the pedestrian trajectories in a crowd based on this formulation.

II. LEAST-EFFORT MODEL

A person's caloric expenditure rate, R, can be well approximated by a quadratic function of their instantaneous speed [3, 4]. In this work we use the approximation provided by Whittle [4]: $R = e_w|\mathbf{v}|^2 + e_s$, where the parameters of e_w and e_s can vary based on gender, age, and fitness level. This function was derived empirically by fitting a curve to data extracted from oxygen consumption of participants walking on a treadmill at various speeds.

For any given trajectory, integrating this caloric rate function over the trajectory will result in an estimate of the total calories a human would expend by traversing the trajectory. This leads to the following equation for the energy expended by a person moving along a path Π:

$$E(\Pi) = m \int_{\Pi} (e_w|\mathbf{v}|^2 + e_s)dt, \qquad (1)$$

where m is the person's mass, e_w captures how efficiently calories are used, and e_s is a person's rate of energy consumption when standing still.

Based on this model, a person will be walking most efficiently when Eq. (1) is optimized per unit distance (Fig. 1). This happens with a path of a constant speed of $\sqrt{e_s/e_w}$. For the average adult male $e_w = 1.26$ and $e_s = 2.23$ [4], which corresponds to a speed of 1.33 m s^{-1}. This matches the measured average walking speed for humans in low density environments [23]. In other words, a least effort analysis correctly predicts that people in an unconstrained environment will take the shortest path to their goal at their optimal speed.

In a crowded environment, however, nearby humans and obstacles result in additional constraints on an individual's motion. The strongest of these constraints is that two people cannot share the same physical space. Additionally, humans tend to avoid collisions in an anticipatory manner, reacting to the collisions before they occur [21]. This can result in a need to constantly adjust paths to avoid collisions well ahead of time to account for the potential actions of others. In other words, humans tend to choose velocities that will result in collision-free motion with respect to other nearby people and obstacles.

To capture these two aspects of human navigation, we propose a model in which each individual in the crowd is modeled as a virtual agent that attempts to find the minimum energy path to its goal while avoiding collisions. We model the tendency to anticipate collisions as a restriction on the set of permissible velocities an agent can take to include only those which result in collision-free paths

for the near future. Here we denote these velocities as PV (Fig. 2 - white region). Our formulation assumes each individual chooses the velocity from this set that is expected to minimize the energy described by Eq. (1). To achieve this minimization, we first express the set of potential velocities PV using a set of linear constraints on the velocities of each agent (Fig. 2). This set can be computed efficiently using geometric optimization techniques. In the remainder of this section we present formally the method by which this set PV can be generated and the optimal velocity computed for each agent.

A. Optimization Formulation

We represent agents as a hard disk with a fixed radius r. Following the methods proposed in Berg et al. [25], we define PV as a intersection of several linear constraints on an agent's velocity, one constraint for each neighboring agent. Given an agent A, for each neighboring agent B, we compute the constraint on A's velocity by first computing the minimum change in the relative velocity between A and B needed to avoid collision for at least τ seconds. This change in velocity is denoted as the vector $\mathbf{u}$. We then constrain A's velocity to change by at least $\frac{1}{2}\mathbf{u}$ (with the assumption B will likewise avoid the other half of the collision). Therefore, given A has a current velocity of $\mathbf{v}_A^{\text{cur}}$, the permitted velocities given B are:

$$PV_{A|B} = \{\mathbf{v} : (\mathbf{v} - (\mathbf{v}_A^{\text{cur}} + \frac{1}{2}\mathbf{u})) \cdot \mathbf{u} \geq 0\}. \quad (2)$$

The boundary of this set is a line which goes through the point $(\mathbf{v}+\frac{1}{2}\mathbf{u})$ with the slope $\mathbf{u}^{\perp} = (\mathbf{u}.y, -\mathbf{u}.x)$. A similar formulation can handle avoidance of obstacles with the exception that obstacles can not be expected to reciprocate in avoiding collisions and therefore the entire vector $\mathbf{u}$ must be accounted for. Therefore, for an obstacle O:

$$PV_{A|O} = \{\mathbf{v} : (\mathbf{v} - (\mathbf{v}_A^{\text{cur}} + \mathbf{u})) \cdot \mathbf{u} \geq 0\}. \quad (3)$$

The union of these linear velocities constraints across all agents forms PV (Fig. 2). Formally:

$$PV = \bigcap_{B \neq A} PV_{A|B} \cap \bigcap_{O} PV_{A|O}. \quad (4)$$

We can now model the PLE notion of the collision-free path taking the least caloric energy as:

$$\textbf{Minimize}\, E(\Pi)\ s.t.\ \mathbf{v}^{init} \in PV, \quad (5)$$

where agents are limited to paths whose initial velocity, $\mathbf{v}^{init}$, lies with the set of non-colliding velocities PV. Solving this equation produces a model for crowd motion which can be summarized as: *each agent finds the path, Π, with an initially velocity $\mathbf{v}^{init}$ from the permitted velocities PV, which minimizes the expected biomechanical effort to reach the goal.*

In practice people can only avoid other agents and obstacles that they are aware of. For the results in this paper we represent the region of awareness as a circle of radius 10m, centered around the agent. Other, anisotropic, models are also possible as our method is independent of the underlying sensing model.

B. Geometric Solution

We can now compute trajectories by solving Eq (5) for each agent. As a simplifying assumption, we restrict ourselves to paths Π which can be represented by two linear segments. The first segment corresponds to a motion that avoids collisions with nearby obstacles and other individuals, and the second segment leads the agent directly to its goal position (Fig. 2 dotted line). We assume the avoidance segment takes τ seconds at an initial velocity of $\mathbf{v}$. We can compute the exact effort along this path as follows: Given an individual's current position, $\mathbf{p}$, and goal position, $\mathbf{G}$, we use Eq. (1) to compute the expected energy along a path as:

$$E(\mathbf{v}) = \tau(e_w|\mathbf{v}|^2 + e_s)m + 2|\mathbf{G} - \mathbf{p} - \tau\mathbf{v}|\sqrt{e_s e_w}m. \quad (6)$$

By combining Eq. (5) and Eq. (6), we can now define our Least Effort model for trajectory computation and motion in crowds as:

$$\textbf{Minimize}\, E(\mathbf{v}^{new})\ s.t.\ \mathbf{v}^{new} \in PV. \quad (7)$$

We note that Eq. (7) can be solved efficiently by exploiting the convexity of the energy function, E, and the convexity of the set of potential velocities, PV as described in in Ref. [26]. We use a linear programming type solution, where each linear segment on boundary of PV is optimized for sequentially.

Specifically, we first find the velocity that minimizes Eq. (6) which we denote as $\mathbf{v}^{opt}$. For Eq. (6), this point can be found analytically through differentiation. For each linear boundary segment of PV, we then check if $\mathbf{v}^{opt}$ is a permitted velocity. If it is not a permitted we find the optimal velocity along the linear boundry. This new point now serves as $\mathbf{v}^{opt}$, and this process is repeated for each remaining segment of PV. The final value of $\mathbf{v}^{opt}$ will be the point that minimizes Eq. (7).

This process is repeated for each agent to compute the optimal velocity, $\mathbf{v}^{opt}$, for that agent. All agent positions are then updated using Eulerian integration of their velocity over discretized time-steps (0.1s in the results below). This process is repeated until each agent reaches its goal position. As discussed in Ref. [25] and Ref. [26], this general method for collision avoidance will lead to provably smooth and collision free paths (provided there is sufficient free space for agents to maneuver). This adds to the generality of our model by alleviating the need to

FIG. 3: (Color online) Stills from a simulation of humans walking through a narrow passage, taken at 15 second intervals. There is initially jamming at the passage (a), followed by a semi-circular arch forming around the exit (b). Once through the passage, individuals do not immediately spread out, but leave an empty space or "wake" behind the obstacles (c).

tune specific parameters to find smooth or collision free paths; rather free parameters can be used to capture the naturally occurring variation in human motion. Additionally, because the implicit cooperation between agents (the results of avoiding only $\frac{1}{2}\mathbf{u}$) large timesteps can be used while still maintaining collision free motion between agents [25].

Our resulting model has three free parameters to describe each agent: the agent's radius, r, and the parameters e_s and e_w in their energy function which define their preferred velocity.

C. Global Navigation

In cases when an agent's goal is not immediately visible, we use a roadmap (a graph of connected, mutually visible, intermediate goals) to select a path of intermediate goals for an agent. The agent then navigates via these intermediate goals along the way to its ultimate destination [25, 26]. We form this roadmap by randomly sampling potential, collision-free positions to select intermediate goals and then connecting mutually visible intermediate goals (whose direct between them does not pass through walls) to create a graph with the intermediate goals as nodes and the path between these goals as edges. Each edge is weighted by the expected caloric energy needed to traverse the link. We use standard graph search techniques to find the series of intermediate goals which forms the path of least expect effort to reach an agent's final goal [27]. The next visible of these intermediate goals serves as an agent's goal, $\mathbf{G}$, in Eq. (6).

Source code implementing these collision avoidance and global navigation techniques are provided online [28].

III. RESULTS

The validity of the model described in Sec. II can be analyzed in several respects. First, we examine the emergent phenomena generated by the model. These are effects which are not explicitly accounted for in the formulation, but reliably occur in simulations due to the interaction between agents. Secondly, we perform a quantitative analysis of how closely our simulated results match data collected about real-word crowd flows and paths taken by humans in controlled studies. Finally, we show results from simulations of complex scenarios consisting of thousands of independent agents and hundreds of obstacles.

A. Emergent Phenomena

We have analyzed several different crowd movement patterns and other emerging behaviors that arise from our Least-Effort model and compared them to observed phenomena in real crowds. For example, simulated individuals tend to dynamically form emergent lanes when they are moving in bi-directional flows as demonstrated in Fig. 4. In this scenario two groups of agents are given goals corresponding to a horizontal movement in opposite directions along the x-axis. In the process of reaching their goals, agents naturally self-organize into lanes. This is a result of the fact that agents spend fewer calories by joining existing lanes of people moving with a similar direction and speed. This allows individuals to move at their most energy efficient speed without having to slow down to avoid collisions and thereby minimize the total individual effort. This emergent lane formation has been commonly reported in observations of real world crowds [10, 23, 29].

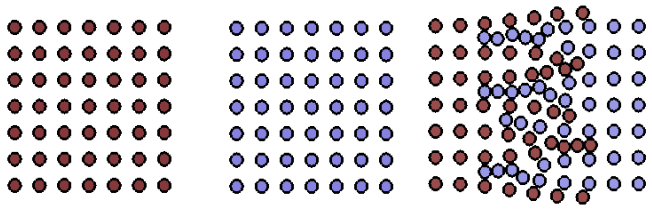

(a) Initial Conditions (b) Lane Formation

FIG. 4: (Color online) Lane Formation. (a) Two opposing groups of agents, (dark) red and (light) blue, have opposing initial conditions with goals past each other. (b) As the groups approach the agents naturally form into small coherent lanes reducing the overall effort of each individual.

Our model is also able to reproduce observed human behavior at narrow passages. The scenario shown in Fig. 3 highlights many of these behaviors. Here, each agent

is given a goal horizontally along the x-axis beyond the narrow passage. The simulated agents tend to jam in the congestion that forms at a narrow passage as they attempt to avoid colliding with other individuals who are nearby. This also leads to semi-circular arching around the passage as the individuals try to come as close as possible to the exit in order to minimize time spent in congestion. These phenomena of jamming, congestion, and arching around exits have all been reported in studies of real human crowds [23, 30].

The process of each individual minimizing his or her caloric energy also allows our model to capture several other common crowd phenomena. For example, obstacles in a crowd's path create an open space behind them which people do not immediately fill (Fig. 3, right panel). This is known as the wake effect [29] as it is reminiscent of flow separation regions in fluids. In such regions the agents tend to choose a direct path towards the goal as it is more efficient overall than filling in the free space behind an obstacle.

Energy minimization also explains overtaking behavior seen in crowds. As shown in Fig. 1, moving slower than the optimal speed is inefficient. Individuals with higher optimal velocity will therefore overtake the slower ones, minimizing their overall effort. Another related phenomenon is congestion avoidance. Taking paths which avoid regions of high density, slow moving individuals often results in using less caloric energy than slowing down and moving through the congestion. Simpler simulation methods such as finding the shortest or quickest path fails to reproduce such effects.

B. Flow Analysis

Further validation of our biomechanically-inspired model of crowd motion can be performed by comparing predictions from the simulation to actual data. For example, several recent studies have analyzed human exit times through doorways of various widths [31–34].

To compare our simulation results to these studies we created a scenario similar to those of the above studies. Several simulations were run where approximately 100 simulated agents are given a goal of a point 10m outside the room centered along the exit's midpoint. For each run the width of the room's exit was varied from 0.8m to 1.4m. Fig. 5 summarizes this simulation set-up.

Fig. 6 compares the flow rate predicted by our least-effort simulations and flow rates measured on real humans. The predicted flow rates lie within the range of flows reported for humans for a range of exit widths.

Another aspect of human flow is the well established correlation between increased density and slower speeds known as the fundamental diagram [35, 36]. Our model shows a similar trend. As an example, we initialize agents with the positions and velocities reported in several timesteps of the Bottleneck benchmark in [36] and plot the predicted speed of each agent as a function of density (Fig. 7). While there is variation in the agents' speeds at any density, in general, agents in high density regions move significantly slower than those in low density regions. The blue line in Fig. 7 shows a quadratic fit of the data, this fit closely matches the fundamental diagram established by Weidmann [35].

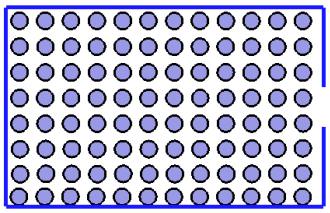

FIG. 5: (Color online) Flow Analysis Scenario. 96 agents are placed in a room of dimension 5m x 8m. Agents are given a goal outside the room which requires them to pass through the exit on the right wall. The experiment is repeated for various exit widths varying from 0.8m to 1.4m.

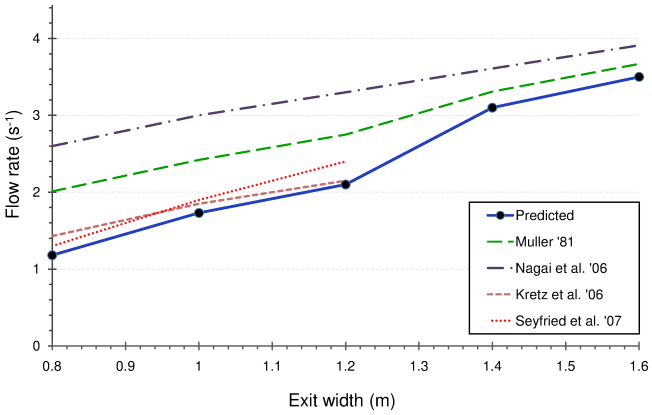

FIG. 6: (Color online) Real and Simulated Flow Rates. A comparison of the effect of exit width on the flow for real (dashed lines) and simulated (solid line) humans. Agents simulated with our model exhibit similar flow as real humans.

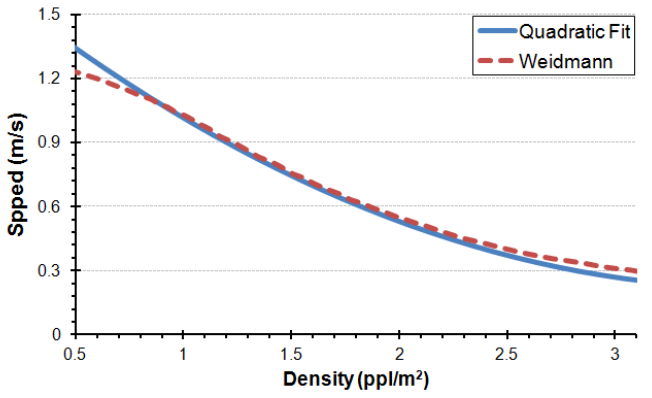

FIG. 7: (Color online) The fundamental diagram comparing agent speeds vs their local density (solid line) matches the relationship established by Weidmann (dashed line) [35].

C. Path Comparison

In addition to comparing real and predicted flows, we can also compare the paths predicted by our method to those of real people walking in similar condition. Here we use data from two scenarios gathered at [37] and presented in Ref. [22].

The first scenario involved two people standing about 6m apart and being instructed to exchange places. Fig. 8 shows the mean and standard deviation of the participants' paths. In this figure all the paths have been normalized so that "forward" corresponds to the positive x-axis. Overlaid on the actual human paths is the path predicted by our method (r=.28m). The path predicted by our method falls within the variation of the human paths and closely matches the mean of the human paths.

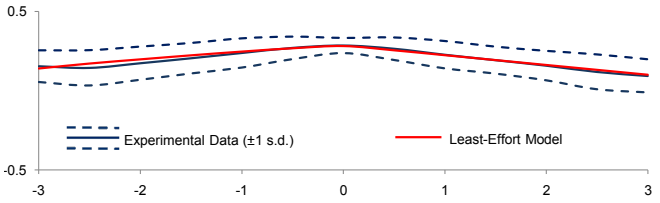

FIG. 8: (Color online) Paths of two humans passing each other. Our model's path (light solid line) matches very closely with the the mean of the human paths (dark solid line), and within one standard deviation of human paths (dashed lines).

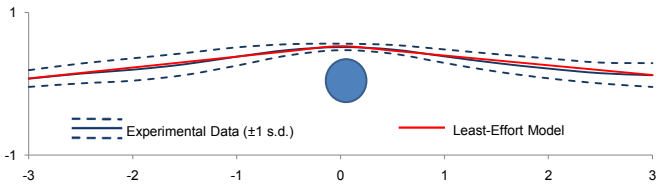

FIG. 9: (Color online) Paths taken past a static obstacle (circle). Our model's path (light solid line) matches very closely with the the mean of the human paths (dark solid line), and within one standard deviation of human paths (dashed lines).

In the second scenario (Fig. 9) we validate the paths from our model against those of real humans when walking around a static obstacle. Again, the path predicted by our model lies within the variation seen in human paths and is close to the mean of the human paths.

D. Complex Scenarios

The simplicity of our algorithm allows us to produce computationally efficient implementations capable of simulating large scale crowd behavior in real time. Because of the underlying efficiency of our approach, we are able to use this model to generate realistic crowd behaviors for complex, real-world scenarios.

One of the key challenges in simulating complex environments is to avoid collisions of the agents with each other and between the agents and the obstacles in the environment. Our method is scalable and can handle complex scenarios involving thousands of virtual agents. In these complex scenarios, the constrained optimization framework discussed in Sec. II. successfully avoids collisions between agents and with obstacles while still navigating agents to their goal. Visualized simulations generated by our least-energy model in a variety of scenarios can be found online at http://gamma.cs.unc.edu/LeastEffort/.

FIG. 10: (Color online) Comparison of Real (top) and Virtual (bottom) Shibuya Crossing. The modeled individuals show a similar pace and self-organization as the real pedestrians.

Finally, we show a comparison between virtual and real crowds in the same scenario. Here we compare a simulated crossing to real footage taken at the five-way scramble crossing outside Shibuya Metro Station in Tokyo (Fig. 10). The bottom panel shows a virtual recreation of the crossing; the top is a still from a video captured at a similar angle. The real-world video and simulations show important similarities in both pace and style. Importantly, this scenario demonstrates phenomena such as lane formation in a natural setting.

IV. SUMMARY AND FUTURE WORK

In summary, we have introduced a new computational model to simulate crowds that display collective behaviors formed by individual trajectories. By combining fundamental biomechanical measurements and the Principle of Least Effort we were able to develop a crowd simulation system based on constrained energy minimization. We have validated our model by comparing the predicted results with data from real-world crowds and have shown that it can accurately model humans paths, crowd flows, and emergent behaviors.

While we have shown that constrained caloric energy minimization can successfully reproduce typical crowd behaviors, there are still scenarios which are not currently well modeled by this approach. For example, there are social and psychological factors, such as running when panicked, that can not be captured simply in terms of minimizing the biomechanical energy of locomotion. Additionally, different people do not always take the exact same path, but rather exhibit variations which come from differences in personality and style.

Looking forward, we conjecture that our approach can be extended to eventually model several of these sociological and psychological factors, as well capture some of the variations seen in humans. Accounting for factors such as discomfort in dark areas or close to walls could further enhance our approach. Such a model could be used to analyze crowd flows in various environments and assist in predicting and controlling crowds in large assemblies.

Additionally, we would like to study how our least-effort model compares to other optimization-based or predictive approaches. Such a study would ideally focus on highly discriminative scenarios such as two pedestrians approaching at various angles.

ACKNOWLEDGMENTS

We are thankful to Jur van den Berg and Brian Skinner for useful discussion and help with the manuscript. This work was supported by ARO Contract W911NF-04-1-0088, NSF awards 0917040, 0904990, 100057 and 1117127, and Intel.

[1] G. Zipf, *Human behavior and the principle of least effort: An introduction to human ecology* (Hafner, New York, 1965).
[2] V. Inman, H. Ralston, F. Todd, and J. Lieberman, *Human walking* (Williams & Wilkins, 1981), ISBN 068304348X.
[3] R. Browning and R. Kram, Obesity **13**, 891 (2005).
[4] M. Whittle, *Gait analysis: an introduction* (Butterworth-Heinemann Medical, 2002), ISBN 0750652624.
[5] A. Crooks, C. Castle, and M. Batty, Computers, Environment and Urban System **32**, 417 (2008).
[6] S. Hoogendoorn and P. Bovy, Transportation Research Part B: Methodological **38**, 169 (2004).
[7] R. Hughes, Annual review of fluid mechanics **35**, 169 (2003).
[8] R. L. Hughe, Transportation Research Part **36**, 507 (2002).
[9] D. Helbing, I. Farkas, and T. Vicsek, Nature **407**, 487 (2000), ISSN 0028-0836.
[10] D. Helbing, L. Buzna, A. Johansson, and T. Werner, Transportation science **39**, 1 (2005).
[11] W. J. Yu, R. Chen, L. Y. Dong, and S. Q. Dai, Phys. Rev. E **72**, 026112 (2005).
[12] M. Chraibi, A. Seyfried, and A. Schadschneider, Phys. Rev. E **82**, 046111 (2010).
[13] C. Reynolds, in *Proceedings of the conference on Computer graphics and interactive techniquesiques (SIGGRAPH)* (ACM, 1987), pp. 25–34, ISBN 0897912276.
[14] T. Kretz, Journal of Statistical Mechanics: Theory and Experiment **2009**, P03012 (2009).
[15] M. Muramatsu and T. Nagatani, Physica A: Statistical Mechanics and its Applications **275**, 281 (2000).
[16] D. Hartmann, New Journal of Physics **12**, 043032 (2010).
[17] A. Johansson, D. Helbing, and P. B. Shukla, Advances in Complex System **10**, 271 (2008).
[18] W. Yu and A. Johansson, Phys. Rev. E **76**, 046105 (2007).
[19] A. Schadschneider, D. Chowdhury, and K. Nishinari, *Stochastic Transport in Complex Systems: From Molecules to Vehicles* (Elsevier, 2011).
[20] S. Paris, J. Pettré, and S. Donikian, in *Computer Graphics Forum* (2007), vol. 26, pp. 665–674.
[21] J. Pettré, J. Ondrej, A.-H. Olivier, A. Cretual, and S. Donikian, in *Proceedings of the 2009 ACM SIGGRAPH/Eurographics Symposium on Computer Animation* (ACM, 2009).
[22] M. Moussaïd, D. Helbing, and G. Theraulaz, Proceedings of the National Academy of Sciences **108**, 6884 (2011).
[23] H. Klüpfel, M. Schreckenberg, and T. Meyer-König, Traffic and Granular Flow pp. 357–372 (2005).
[24] B. Maury and J. Venel, Comptes Rendus Mathematique **346**, 1245 (2008).
[25] J. van den Berg, S. Guy, M. Lin, and D. Manocha, International Symposium on Robotics Research, Springer Tracts in Advanced Robotics **70**, 3 (2011).
[26] S. J. Guy, J. Chhugani, S. Curtis, M. C. Lin, P. Dubey, and D. Manocha, in *Proceedings of the Symposium on Computer Animation* (ACM, 2010).
[27] S. M. LaValle, *Planning Algorithms* (Cambridge University Press, Cambridge, U.K., 2006), available at http://planning.cs.uiuc.edu/.
[28] *http://gamma.cs.unc.edu/RVO2/*.
[29] G. Still, Ph.D. thesis, Coventry, UK: Warwick University (2000).
[30] V. Predtetschenski and A. Milinski, *Personenströme in Gebäuden-Berechnungsmethoden für die Projektierung* (Staatsverlag der Deutschen, 1971).
[31] K. Müller, Ph.D. thesis, Technische Hochschule Otto von Guericke Magdeburg (1981).
[32] R. Nagai, M. Fukamachi, and T. Nagatani, Physica A: Statistical Mechanics and its Applications **367**, 449 (2006), ISSN 0378-4371.
[33] T. Kretz, A. Grünebohm, and M. Schreckenberg, Journal of Statistical Mechanics: Theory and Experiment p. P10014 (2006).
[34] A. Seyfried, O. Passon, B. Steffen, M. Boltes, T. Rupprecht, and W. Klingsch, Transportation Science **43**, 395 (2009), ISSN 1526-5447.
[35] U. Weidmann, Strasse und Verkehr **78**, 161 (1992).
[36] A. Seyfried, M. Boltes, J. Kähler, W. Klingsch, A. Portz, T. Rupprecht, A. Schadschneider, B. Steffen, and A. Winkens, Pedestrian and Evacuation Dynamics (2008).

[37] *Centre de Recherches sur la Cognition Animale, CNRS, Toulouse, France* (2011).